

Renormalized Singles Green's Function in the T-Matrix Approximation for Accurate Quasiparticle Energy Calculation

Jiachen Li, Zehua Chen, and Weitao Yang*

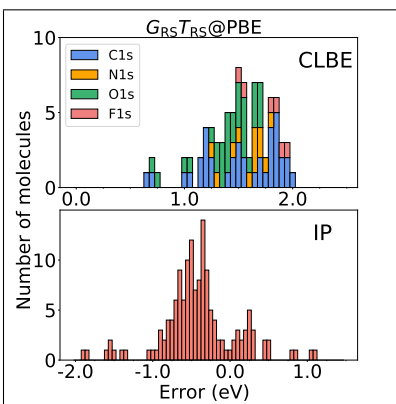
Department of Chemistry, Duke University, Durham, NC 27708, USA

E-mail: weitao.yang@duke.edu

Abstract

We combine the renormalized singles (RS) Green’s function with the T-Matrix approximation for the single-particle Green’s function to compute quasiparticle energies for valence and core states of molecular systems. The $G_{\text{RS}}T_0$ method uses the RS Green’s function that incorporates singles contributions as the initial Green’s function. The $G_{\text{RS}}T_{\text{RS}}$ method further calculates the generalized effective interaction with the RS Green’s function by using RS eigenvalues in the T-Matrix calculation through the particle-particle random phase approximation. The $G_{\text{RS}}T_{\text{RS}}$ method provides significant improvements over the one-shot T-Matrix method G_0T_0 as demonstrated in calculations for GW100 and CORE65 test sets. It also systematically eliminates the dependence of G_0T_0 on the choice of density functional approximations (DFAs). For valence states, the $G_{\text{RS}}T_{\text{RS}}$ method provides an excellent accuracy, which is better than G_0T_0 with Hartree-Fock (HF) or other DFAs. For core states, the $G_{\text{RS}}T_{\text{RS}}$ method correctly identifies desired peaks in the spectral function and significantly outperforms G_0T_0 on core level binding energies (CLBEs) and relative CLBEs, with any commonly used DFAs.

Graphical TOC Entry



Keywords

T-Matrix, Self-Energy, Quasiparticle

Quasiparticle (QP) energies constitute one of the most important electronic properties of molecules and materials. Although they can be measured in photoemission and inverse photoemission spectroscopies, the computational study of QP energies plays an important role for understanding electronic structures from basic principles and for molecular and material designs. The *GW* method,¹⁻³ which is developed from Hedin's equations,⁴ is a state-of-art formalism to study QP energies, and charged electronic excitations in molecules⁵⁻¹² and solids.¹³⁻²¹ The success of the *GW* method stems from a clear physical interpretation for QP energies, a favorable computational scaling with respect to the size of systems and a proper description of the screened interaction.¹ The *GW* method is viewed as the "gold standard" for band gap calculations²² for periodic systems, and the *GW* method has been widely used to investigate both valence²³⁻²⁵ and core²⁶⁻²⁸ state properties for molecular systems. Despite enormous successes achieved by *GW* in practical calculations, the most commonly-used *GW* variant, the one-shot method G_0W_0 , still suffers from the strong starting-point dependence. In practice, the G_0W_0 method is usually combined with a preceding Kohn-Sham (KS) density functional theory (DFT) calculation²⁹⁻³¹ calculation. The difference originated from using different density functional approximations (DFAs) can exceed 1 eV for ionization potentials (IPs) and electron affinities (EAs) of molecules^{5,32} and can be even larger than 2 eV for binding energies of solids.³³ Partial or full self-consistent *GW* approaches, such as *evGW* and *scGW* can greatly improve the accuracy and eliminate the starting-point dependence for both valence and core state calculations,^{24,34,35} but inevitably bring additional computational cost.

Another approach in *GW* is using the (RS) Green's function³⁶ as the new starting point, which is denoted as $G_{\text{RS}}W_0$ and $G_{\text{RS}}W_{\text{RS}}$.³⁷ The motivation of the RS Green's function is to use the form of the Hartree-Fock^{38,39} (HF) self-energy to include singles contributions because it captures all the contributions of the single excitations completely, unlike in the commonly used G_0W_0 , which is done perturbatively. The RS as the reference noninteracting single-particle Green's function shares similar thinking as the renormalized singles correction

for correlation energies.^{40,41} The HF Green’s function itself is not a good starting point for G_0W_0 .^{36,42} However, the renormalization process of forming the HF self-energy with DFA orbitals significantly improves the accuracy and eliminates the dependence on orbital energies of the DFA.³⁶ Furthermore, the incorporation of singles contributions, using RS eigenvalues with KS orbitals has been shown to lead to corrections to the underestimation of excitation energies from the particle-hole random phase approximation (phRPA) based on commonly used KS DFA.⁴³ The underestimated excitation energies from the phRPA at DFA levels erroneously transfer spectral weights from desired QP peaks to satellites.⁴⁴ The improved phRPA excitation energies lead to a unique solution of the QP equation in the core region.³⁷ The renormalization step is a much less computational-demanding step than solving the phRPA equation and formulating the self-energy. Developed in the first paper on the RS Green’s function, the $G_{RS}W_0$ method uses the RS Green’s function as the new starting point but calculates the screened interaction with the KS Green’s function and it leads to considerable improvements over G_0W_0 for IPs and EAs.³⁶ Then the $G_{RS}W_{RS}$ method that also uses the RS Green’s function in the screened interaction has been shown to provide better results than G_0W_0 for core level binding energies (CLBEs) and it reproduces correct behaviors for spectral functions.³⁷

In this paper, we introduce the RS Green’s function to the counterpart of GW in the particle-particle (pp) channel, which is the T-Matrix method. The T-Matrix approximation or the Bethe-Goldstone approximation was originally introduced to treat the interaction of complex nuclei.^{45–49} The T-Matrix method was used to describe electronic structures of the Hubbard model.^{50–54,54} It has also been applied to study periodic systems in material science, including satellites,^{55,56} double excitations^{57,58} and spin-flip excitations of metals.^{59,60} It has been shown that the T-Matrix method works well for the low-density limit, where the screening effect has less impact and the GW approximation fails.^{48,61}

Recently, the T-Matrix method was introduced to predict accurate QP spectra of molecules,⁶² motivated by desirable improvements on predicting excitation energies of the particle-particle

random phase approximation (ppRPA)⁶³⁻⁶⁵ over the phRPA.^{66,67} In the T-Matrix approximation, the self-energy is formulated with a four-point generalized effective interaction $T(1, 3; 2, 4)$ instead of the two-point screened interaction $W(1, 2)$. The advantage of using the four-point generalized effective interaction is that, the self-energy includes electron exchange interactions and it is exact up to second order in the bare interaction, while in the GW method the self-energy does not have these properties. Similar to the GW approximation that is based on the phRPA, the T-Matrix approximation has been formulated with the pairing excitation eigenvalues and eigenvectors of the ppRPA matrix.⁶² Comparing with the GW approximation containing correlated electron-hole pairs in the screened interaction, which are drawn as ring diagrams, the T-Matrix approximation describes correlations of two electrons or through Coulomb and exchange interactions, which can be drawn as ladder diagrams. Thus the T-Matrix approximation can be considered as the pp counterpart of GW . In the first application of the T-Matrix approximation to molecular systems, the one-shot calculation of the T-Matrix approximation (denoted as G_0T_0) was carried out.⁶² It was shown that the T-Matrix approximation has very good accuracy, with much better agreements with experimental valence states than the bare KS eigenvalues. However, as will be shown below, the QP equation of the G_0T_0 has multiple solutions in the core region, which gives erroneous CLBEs. Beside the problematic behavior in computing CLBEs, the G_0T_0 method also suffers from the strong dependence of the starting DFAs.⁶² For valence and core calculations, $G_0T_0@HF$ predicts accurate results with a mean absolute error (MAE) of 0.54 eV but $G_0T_0@PBE$ gives a relatively large MAE of 1.90 eV. Motivated by the success of using the RS Green's function in GW ,³⁶ in this work, we introduce the RS Green's function to the T-Matrix method, and investigate valence and core state properties of molecular systems.

We first review the self-energy from the GW approximation and the T-Matrix approximation. In the time domain, the real-space GW self-energy is expressed as the product of

the Green's function and the two-point screened interaction

$$\Sigma^{GW}(1, 2) = iG(1, 2)W(1, 2), \quad (1)$$

where the variables 1, 2 are shorthand notations for combined space-time-spin variables.^{1,4} The screened interaction W can be formulated with eigenvalues and eigenvectors of the phRPA matrix.⁶⁸

The T-Matrix approximation generalizes the two-point interaction $W(1, 2)$ in GW to a four-point effective interaction $T(1, 3; 2, 4)$, which makes the T-Matrix self-energy an integral of the Green's function and T

$$\Sigma^T(1, 2) = i \int d3d4 G(4, 3)T(1, 3; 2, 4). \quad (2)$$

In terms of diagrams, the T-Matrix approximation corresponds to an infinite summation of ladder diagrams with corresponding exchange terms.^{1,46,48} Comparing to the infinite summation of ring diagrams in GW , which represents screened interactions, the ladder diagrams indicate scattering interactions between pairs of particles and between pairs of holes. The T-Matrix approximation is exact up to the second order because of its proper description of second-order exchange diagrams, which are missing in the GW approximation.

The Fourier transform of the correlation part of the self-energy Σ^T in the frequency domain is given as⁶²

$$\begin{aligned} \Sigma_c^T(p, q, \omega) = & \sum_m \sum_i \frac{\langle pi | \chi_m^{N+2} \rangle \langle qi | \chi_m^{N+2} \rangle}{\omega + \epsilon_i - \omega_m^{N+2} + i\eta} \\ & + \sum_m \sum_a \frac{\langle pa | \chi_m^{N-2} \rangle \langle qa | \chi_m^{N-2} \rangle}{\omega + \epsilon_a - \omega_m^{N-2} - i\eta}. \end{aligned} \quad (3)$$

Here, we use i, j, k, l for occupied orbitals, a, b, c, d for virtual orbitals, p, q, r, s for general orbitals and m for the index of the excitation from the ppRPA. The transition density in

Equation.3 is

$$\langle pi|\chi_m^{N+2}\rangle = \sum_{c<d} \langle pi||cd\rangle X_{cd}^{N+2,m} + \sum_{k<l} \langle pi||kl\rangle Y_{kl}^{N+2,m} \quad (4)$$

$$\langle pa|\chi_m^{N-2}\rangle = \sum_{c<d} \langle pa||cd\rangle X_{cd}^{N-2,m} + \sum_{k<l} \langle pa||kl\rangle Y_{kl}^{N-2,m}, \quad (5)$$

where $X_m^{N\pm 2}$, $Y_m^{N\pm 2}$ and $\omega_m^{N\pm 2}$ are two-electron addition/removal eigenvectors and eigenvalues of the ppRPA matrix equation^{63,64,69}

$$\begin{bmatrix} \mathbf{A} & \mathbf{B} \\ \mathbf{B}^T & \mathbf{C} \end{bmatrix} \begin{bmatrix} \mathbf{X} \\ \mathbf{Y} \end{bmatrix} = \omega^{N\pm 2} \begin{bmatrix} \mathbf{I} & \mathbf{0} \\ \mathbf{0} & -\mathbf{I} \end{bmatrix} \begin{bmatrix} \mathbf{X} \\ \mathbf{Y} \end{bmatrix}, \quad (6)$$

with

$$A_{ab,cd} = \delta_{ac}\delta_{bd}(\epsilon_a + \epsilon_b) + \langle ab||cd\rangle, \quad (7)$$

$$B_{ab,kl} = \langle ab||kl\rangle, \quad (8)$$

$$C_{ij,kl} = -\delta_{ik}\delta_{jl}(\epsilon_i + \epsilon_j) + \langle ij||kl\rangle. \quad (9)$$

In above equations, the antisymmetrized two-electron integral $\langle pq||rs\rangle$ is defined as

$$\langle pq||rs\rangle = \langle pq|rs\rangle - \langle qp|rs\rangle \quad (10)$$

$$= \int dx_1 dx_2 \frac{\phi_p^*(x_1)\phi_q^*(x_2)(1 - \hat{P}_{12})\phi_r(x_1)\phi_s(x_2)}{|r_1 - r_2|} \quad (11)$$

where x indicates both spatial and spin coordinates.

In the G_0T_0 approach, the QP energies are calculated by the linearized QP equation⁶²

$$\epsilon_p^{\text{QP}} = \epsilon_p^{\text{SCF}} + Z_p \langle p|\Sigma^T(p, p, \epsilon_p^{\text{SCF}}) - v_{xc}|p\rangle, \quad (12)$$

where the linearization factor Z_p is

$$Z_p = \left(1 - \frac{\partial \Sigma^T(p, p, \omega)}{\partial \omega} \Big|_{\omega=\epsilon_p^{\text{SCF}}} \right)^{-1}. \quad (13)$$

Here $\{\epsilon_p^{\text{SCF}}\}$ is a set of KS eigenvalues from the self-consistent field (SCF) DFA calculation.

The one-shot G_0T_0 method has an undesired dependence on the choice of the DFA, because the contributions of the singles, namely the effects of electron exchange in Σ^T , are described only in a perturbative manner in Eq.12. The RS approach sums all the contributions of the singles through a one-particle space diagonalization and thus reduces the dependence on the starting DFA, and at the same time uses density matrices from commonly used DFAs.³⁶ We now apply the RS Green's function in the T-Matrix method. To take advantage of the form of the HF self-energy to eliminate the dependence on the orbital energies of the DFA, the RS Green's function is defined as the solution of the two projected equations in the occupied orbital subspace and the virtual orbital subspace³⁶

$$P(G_{\text{RS}}^{-1})P = P(G_0^{-1})P + P(\Sigma_{\text{Hx}}[G_0] - v_{\text{Hxc}})P, \quad (14)$$

and

$$Q(G_{\text{RS}}^{-1})Q = Q(G_0^{-1})Q + Q(\Sigma_{\text{Hx}}[G_0] - v_{\text{Hxc}})Q, \quad (15)$$

where $P = \sum_i^{\text{occ}} |\psi_i\rangle\langle\psi_i|$ is the projection into the occupied orbital space and $Q = I - P$ is the projection into the virtual orbital space. $\Sigma_{\text{Hx}}[G_0]$ means that the HF self-energy consisting of Hartree and exchange parts is constructed from the KS density matrix. Equivalently, the RS Green's function is obtained by using the DFA density matrix in the HF Hamiltonian, namely $H_{\text{HF}}[G_0]$, and solving two projected HF equations in the occupied/virtual subspaces³⁶

$$P(H_{\text{HF}}[G_0])P|\Psi_i^{\text{RS}}\rangle = \epsilon_i^{\text{RS}}P|\Psi_i^{\text{RS}}\rangle, \quad (16)$$

and

$$Q(H_{\text{HF}}[G_0])Q|\Psi_a^{\text{RS}}\rangle = \epsilon_a^{\text{RS}}Q|\Psi_a^{\text{RS}}\rangle. \quad (17)$$

The resulting RS Green's function is diagonal in the occupied and virtual subspaces³⁶

$$G_{nm}^{\text{RS}}(\omega) = \delta_{nm} \frac{1}{\omega - \epsilon_n^{\text{RS}} + i\eta \text{sgn}(\epsilon_n^{\text{RS}} - \mu)}. \quad (18)$$

Here μ is the chemical potential and η is the broadening parameter. The RS Green's function has been implemented in the *GW* calculations in the QM4D package.^{36,70}

We now develop the RS Green's function for the T-Matrix method. In the T-Matrix approximation, we apply the RS Green's function in two ways: $G_{\text{RS}}T_{\text{RS}}$ and $G_{\text{RS}}T_0$. The $G_{\text{RS}}T_0$ approach uses the Green's function as a new starting point and the generalized effective interaction T is calculated with the KS Green's function. During the evaluation of the self-energy, the KS orbitals are used for simplicity, as advocated in the original work of $G_{\text{RS}}W_0$.³⁶ The validity of using just the KS orbitals is further confirmed in present work. In the Supporting Information, it is shown that IPs and CLBEs from $G_{\text{RS}}T_0$ and $G_{\text{RS}}T_{\text{RS}}$ using KS orbitals and RS orbitals provide essentially the same results. The exchange part of the $G_{\text{RS}}T_0$ self-energy and the $G_{\text{RS}}T_{\text{RS}}$ self-energy is the same as G_0T_0 and the correlation part of the $G_{\text{RS}}T_0$ self-energy is

$$\begin{aligned} \Sigma_c^{G_{\text{RS}}T_0}(p, q, \omega) &= \sum_m \sum_i \frac{\langle pi | \chi_m^{N+2} \rangle \langle qi | \chi_m^{N+2} \rangle}{\omega + \epsilon_i^{\text{RS}} - \omega_m^{N+2} - i\eta} \\ &+ \sum_m \sum_a \frac{\langle pa | \chi_m^{N-2} \rangle \langle qa | \chi_m^{N-2} \rangle}{\omega + \epsilon_a^{\text{RS}} - \omega_m^{N-2} + i\eta}. \end{aligned} \quad (19)$$

Here we follow the approximation in the $G_{\text{RS}}W_0$, where DFA orbitals are used for simplicity. As can be seen above, KS eigenvalues in the denominators are simply replaced by RS eigenvalues. The QP equation of $G_{\text{RS}}T_0$

$$\epsilon_p^{\text{QP}} = \epsilon_p^{\text{SCF}} + Z_p \langle p | \Sigma^{G_{\text{RS}}T_0}(p, p, \epsilon_p^{\text{RS}}) - v_{\text{xc}} | p \rangle, \quad (20)$$

which can be linearized by the factor $Z_p = (1 - \frac{\partial \Sigma^c(p,p,\omega)}{\partial \omega}|_{\omega=\epsilon_p^{\text{RS}}})^{-1}$.

The $G_{\text{RS}}T_{\text{RS}}$ approach further calculates the generalized effective interaction T with the RS Green's function, which means RS eigenvalues are used in the ppRPA calculations. The KS orbitals are also used for simplicity without the loss of accuracy (See Ref.³⁶ and the Supporting Information). The self-energy of $G_{\text{RS}}T_{\text{RS}}$ is thus

$$\begin{aligned} \Sigma_c^{G_{\text{RS}}T_{\text{RS}}}(p, q, \omega) = & \sum_m \sum_i \frac{\langle pi | \chi_m^{\text{RS}, N+2} \rangle \langle qi | \chi_m^{\text{RS}, N+2} \rangle}{\omega + \epsilon_i^{\text{RS}} - \omega_m^{\text{RS}, N+2} - i\eta} \\ & + \sum_m \sum_a \frac{\langle pa | \chi_m^{\text{RS}, N-2} \rangle \langle qa | \chi_m^{\text{RS}, N-2} \rangle}{\omega + \epsilon_a^{\text{RS}} - \omega_m^{\text{RS}, N-2} + i\eta}. \end{aligned} \quad (21)$$

Thus the QP equation of $G_{\text{RS}}T_{\text{RS}}$ is

$$\epsilon_p^{\text{QP}} = \epsilon_p^{\text{SCF}} + Z_p \langle p | \Sigma^{G_{\text{RS}}T_{\text{RS}}}(p, p, \epsilon_p^{\text{RS}}) - v_{\text{xc}} | p \rangle, \quad (22)$$

which can be linearized by the factor $Z_p = (1 - \frac{\partial \Sigma^c(p,p,\omega)}{\partial \omega}|_{\omega=\epsilon_p^{\text{RS}}})^{-1}$.

We implemented $G_{\text{RS}}T_{\text{RS}}$ and $G_{\text{RS}}T_0$ methods in QM4D quantum chemistry package⁷⁰ to calculate IPs and CLBEs of molecular systems. As discussed in benchmarks of the GW100 set for *GW* methods,^{23,24} EAs of many molecules in the GW100 set are negatives, where the experimental values are not available. Therefore, we here focus on the discussion of IPs. Results of EAs can be found in the Supporting Information. We use Cartesian basis sets and uses the resolution of identity⁷¹⁻⁷³ (RI) technique to compute two-electron integrals in the T-Matrix method. The broadening parameter η is set as 1.0×10^{-3} A.U. for numerical stability considerations. The convergence criteria is set as 1.0×10^{-5} A.U. in the iterative procedure to solve the QP equation (Eqs. 12, 20 and 22). The convergence with respect to the broadening parameter has been assured and test data can be found in supporting information. The T-Matrix methods are tested with different noninteracting references, including HF and a variety of functionals, such as the generalized gradient approximation (GGA) functional PBE,⁷⁴ and hybrid functionals B3LYP^{75,76} and PBE0.^{77,78} We benchmarked IPs and

EAs of molecules in the GW100 set with def2-TZVPP⁷⁹ basis set and CLBES of molecules in the CORE65 set with def2-TZVP⁷⁹ basis set. We excluded 35 large molecules in the GW100 set and 8 large molecules in the CORE65 set because of their high computational cost. Corresponding RI fitting basis sets⁸⁰ are used. All basis sets are taken from Basis Set Exchange.^{81–83} Experiment values of IPs and EAs are taken from Setten’s work.²³ Experiment values of CLBES are taken from Golze’s work.²⁶ More details and results can be found in the Supporting Information.

We first examine $G_{\text{RS}}T_0$ and $G_{\text{RS}}T_{\text{RS}}$ methods for molecular IP prediction. The IPs are obtained from G_0T_0 , $G_{\text{RS}}T_0$, $G_{\text{RS}}T_{\text{RS}}$ and G_0W_0 based on HF, PBE and PBE0. The MAEs comparing to experiment results can be seen in Table.1. Our G_0T_0 results are consistent with the previous work,⁶² with $G_0T_0@HF$ having the smallest MAE. We also find that G_0T_0 with DFA references can have improved accuracy with some fractions of the Hartree-Fock exchange. As expected, both $G_{\text{RS}}T_0@HF$ and $G_{\text{RS}}T_{\text{RS}}@HF$ show very similar results as $G_0T_0@HF$. The MAEs of $G_{\text{RS}}T_0$ with both PBE and PBE0 are smaller comparing with G_0T_0 . The MAEs are reduced from 1.32 eV and 0.98 eV to 1.03 eV and 0.81 eV when the RS Green’s function is used as the new starting point. The accuracy greatly improves when the generalized effective interaction T is also calculated with the RS Green’s function in the $G_{\text{RS}}T_{\text{RS}}$ approach. The MAEs of $G_{\text{RS}}T_{\text{RS}}$ with PBE and PBE0 are reduced to 0.53 eV and 0.54 eV. In addition to the improved accuracy, the starting point dependence is greatly reduced in the $G_{\text{RS}}T_{\text{RS}}$ approach. This can be seen in Fig.1. For G_0T_0 results, different starting points show distinct error distributions. The error distribution of $G_0T_0@HF$ is more centered around zero than G_0T_0 combining with other DFAs. For $G_{\text{RS}}T_{\text{RS}}$, using PBE or PBE0 as starting points provide very similar distributions, which are also centered. We also find that the distributions of $G_{\text{RS}}T_{\text{RS}}$ methods are in the range of -2.0 eV to 2.0 eV. However, results of As_2 and Br_2 molecules from $G_0T_0@HF$ have absolute errors of 4.11 eV and 3.75 eV, even though $G_0T_0@HF$ has a similar MAE to the $G_{\text{RS}}T_{\text{RS}}$ method. Therefore, the $G_{\text{RS}}T_{\text{RS}}$ method has a better consistency than $G_0T_0@HF$ over the IP test sets.

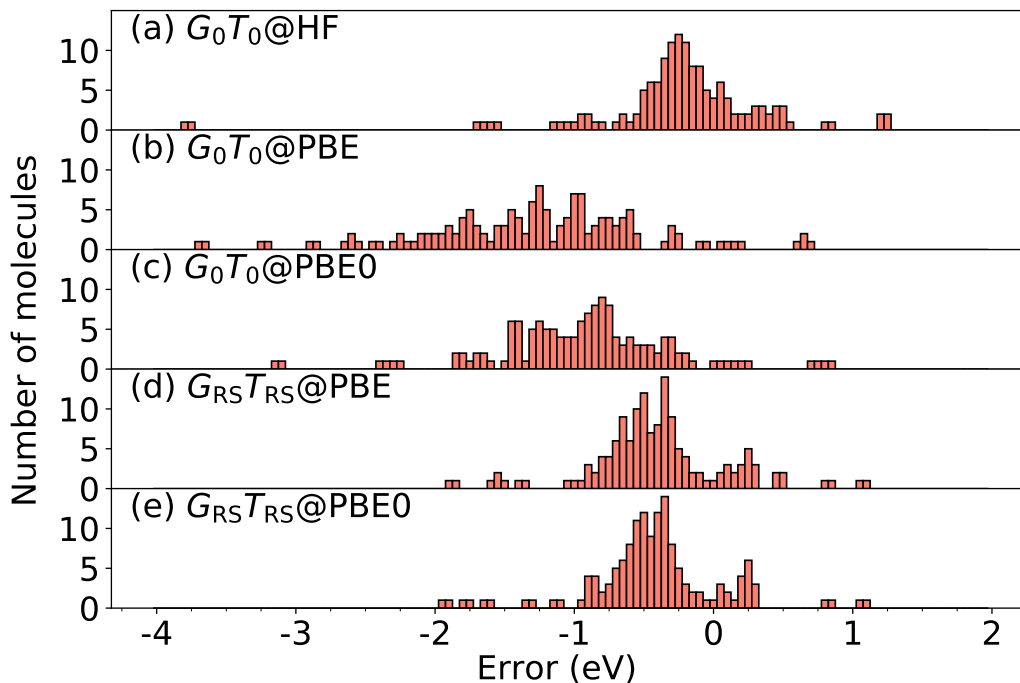


Figure 1: Distributions of errors with respect to the experimental IPs of the GW100 benchmark set from (a) G_0T_0 @HF, (b) G_0T_0 @PBE, (c) G_0T_0 @PBE0, (d) $G_{RS}T_{RS}$ @PBE, (e) $G_{RS}T_{RS}$ @PBE0, where $\text{Error}_i = \text{IP}_i^{\text{theory}} - \text{IP}_i^{\text{exp}}$.

Table 1: Results of IPs in the GW100 set from G_0T_0 , $G_{RS}T_0$, $G_{RS}T_{RS}$ and G_0W_0 based on PBE, PBE0 and HF (eV). "Max Error" means the largest absolute error in the GW100 set predicted by the corresponding method.

	G_0T_0			$G_{RS}T_0$			$G_{RS}T_{RS}$			G_0W_0	
	HF	PBE	PBE0	HF	PBE	PBE0	HF	PBE	PBE0	HF	PBE
MAE	0.52	1.32	0.98	0.56	1.03	0.81	0.56	0.53	0.54	0.57	0.70
Max Error	4.11	3.66	3.08	4.11	3.01	2.67	4.11	1.91	1.84	3.70	2.93

Next we apply $G_{RS}T_0$ and $G_{RS}T_{RS}$ methods to core level calculations. We present CLBE results for molecules in the CORE65 set calculated with G_0T_0 , $G_{RS}T_0$ and $G_{RS}T_{RS}$ combining with different starting points, including PBE, PBE0, B3LYP and HF. The CORE65 set contains C_{1s} , N_{1s} , O_{1s} and F_{1s} excitations from molecules that consist of up to 8 atoms. We excluded 8 large molecules because of computational cost considerations. From Table.2 it can be seen that using PBE as the starting point in G_0T_0 gives the , largest error of around 15.0 eV. The MAE is reduced when hybrid functionals are used as the starting

point. $G_0T_0@PBE0$ and $G_0T_0@B3LYP$ show similar MAEs around 9.0 eV, which are still large. The MAE of $G_0T_0@HF$ is the smallest, which is similar to the conclusion for valence calculations. The MAEs of $G_{RS}T_0$ are reduced from those of G_0T_0 by about 2.0 eV. It can be found that using the RS Green’s function in the T-Matrix further reduces errors for all types of functionals, which are around 1.5 eV. In addition, the starting-point dependence is significantly reduced. All starting points give MAEs smaller than 2.0 eV. This shows that the $G_{RS}T_{RS}$ method has the best accuracy and consistency compared with other methods.

Table 2: MAEs of CLBEs in the CORE65 set from G_0T_0 , $G_{RS}T_0$, $G_{RS}T_{RS}$, G_0W_0 based on PBE, B3LYP, PBE0 and HF (eV).

	PBE	PBE0	B3LYP	HF
G_0T_0	14.97	7.80	9.34	3.74
$G_{RS}T_0$	12.21	6.47	7.55	3.74
$G_{RS}T_{RS}$	1.53	2.06	1.66	3.74
G_0W_0		5.06	5.96	5.67

^a Cartesian def2-TZVP basis set is used. ^b Geometries and reference values are taken from Golze’s work.⁴⁴

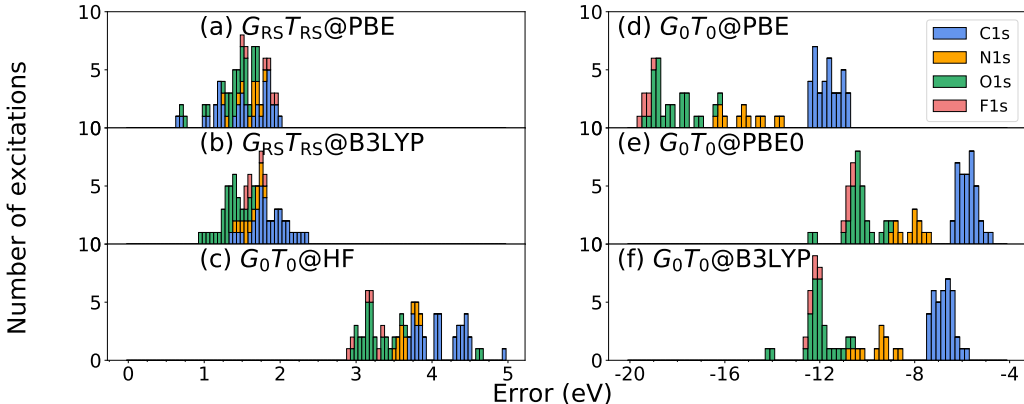


Figure 2: Distributions of errors with respect to the experimental CLBEs in the CORE65 benchmark set from (a) $G_{RS}T_{RS}@PBE$, (b) $G_{RS}T_{RS}@B3LYP$, (c) $G_0T_0@HF$, (d) $G_0T_0@PBE$, (e) $G_0T_0@PBE0$, (f) $G_0T_0@B3LYP$, where $Error_i = CLBE_i^{theory} - CLBE_i^{exp}$. The histograms are stacked.

The distributions of errors with respect to experimental values of CLBE from $G_{RS}T_{RS}$ and G_0T_0 with different starting points are shown in Fig.2. It can be seen that the distributions of $G_{RS}T_{RS}$ methods are the most centered. The distributions of G_0T_0 methods are very different

when different starting points are used. Our calculations indicate that $G_{\text{RS}}T_{\text{RS}}$ overestimate CLBEs only for less than 2.0 eV, which clearly outperforms G_0T_0 (with -20 eV to 3 eV errors). $G_{\text{RS}}T_{\text{RS}}$ combining with different functionals shows similar error distributions. This again indicates that functional dependence is reduced significantly in the $G_{\text{RS}}T_{\text{RS}}$ method.

Table 3: MAEs of relative CLBEs in the CORE65 set from G_0T_0 and $G_{\text{RS}}T_{\text{RS}}$ based on PBE, B3LYP, PBE0 and HF (eV). The relative CLBEs are the shifts with respect to a reference molecule, $\Delta\text{CLBE} = \text{CLBE} - \text{CLBE}_{\text{ref_mol}}$. CH_4 , NH_3 , H_2O and CF_4 have been used as reference molecules for C_{1s} , N_{1s} , O_{1s} and F_{1s} respectively.

	G_0T_0				$G_{\text{RS}}T_{\text{RS}}$			
	PBE	PBE0	B3LYP	HF	PBE	PBE0	B3LYP	HF
C	0.85	0.42	0.41	0.33	0.39	0.29	0.46	0.33
N	1.40	0.78	0.88	0.09	0.19	0.11	0.12	0.09
O	2.29	1.11	1.47	0.22	0.29	0.17	0.21	0.22
F	0.22	0.18	0.11	0.13	0.22	0.09	0.07	0.13

The $G_{\text{RS}}T_{\text{RS}}$ method also provides improvement on predicting relative CLBEs. As can be seen in Table.3, the MAEs of relative CLBEs from $G_{\text{RS}}T_{\text{RS}}$ with all starting points are below 0.50 eV. For N_{1s} , O_{1s} and F_{1s} , $G_{\text{RS}}T_{\text{RS}}$ gives errors that are smaller than 0.3 eV. The starting point dependence in G_0T_0 is clearly shown. $G_0T_0@HF$ provides similar MAEs as $G_{\text{RS}}T_{\text{RS}}$, but G_0T_0 based on other KS starting points can give MAEs exceeding 2.00 eV. The dependence is greatly reduced in $G_{\text{RS}}T_{\text{RS}}$, as the difference of MAEs between different starting points in $G_{\text{RS}}T_{\text{RS}}$ are much smaller than those of G_0T_0 . The good performance of $G_{\text{RS}}T_{\text{RS}}$ is illustrated by the graphical solutions of different approaches in Fig.3. In Fig.3, the solutions of the QP equation is found at intersections between the correlation part of O_{1s} self-energy $\Sigma_{\text{C},1}^{\text{T}}$ and $\omega - \epsilon_{1s} + v_{1s}^{\text{xc}} - \Sigma_{1s}^{\text{x}}$. For $G_0T_0@PBE$, many intersections can be observed in the core region. This means the QP state erroneously transfers spectral weight to satellites, which leads to incorrect QP solutions. This error stems from the underestimation of excitation energies in the ppRPA step at the PBE level. When using RS Green’s function, ppRPA excitation energies are improved, thus satellites shift away from the correct QP states. Only one intersection can be found in the core region, and it is our desired QP state. The

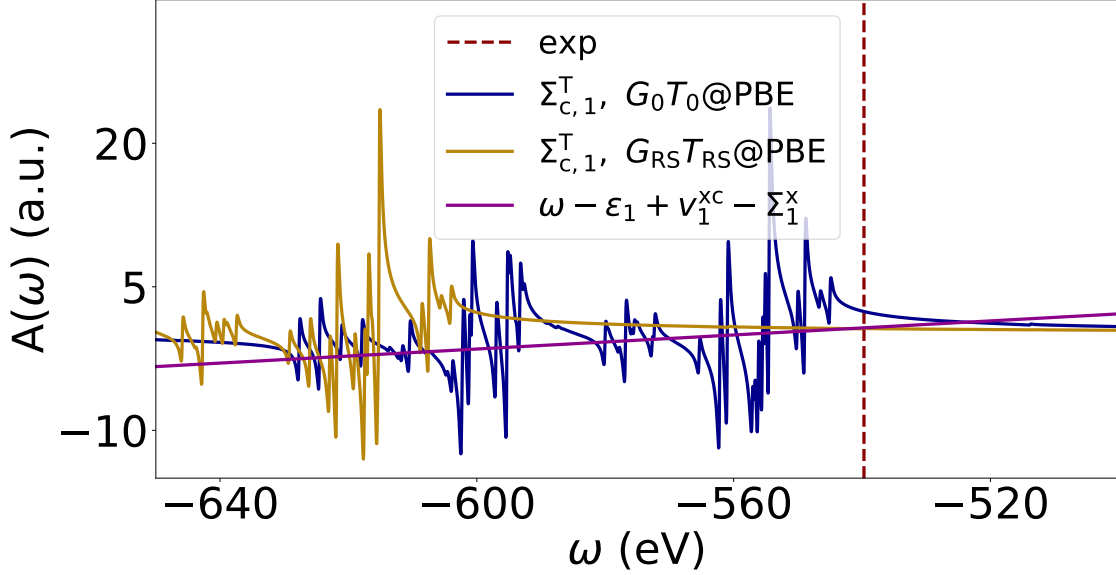


Figure 3: Graphical solutions of O_{1s} excitation in the water molecule from $G_0T_0@PBE$ and $G_{RS}T_{RS}@PBE$. The graphical solutions are found at intersections between $\omega - \epsilon_{1s} + v_{1s}^{xc} - \Sigma_{1s}^x$ (the green line) and the correlation part of O_{1s} self-energy from $G_0T_0@PBE$ (the blue line) or $G_{RS}T_{RS}@PBE$ (the orange line). The vertical red line is the experimental value. def2-TZVP basis set is used.

solutions from different approaches are also reflected in spectral functions, as shown in Fig.4. The equations for computing spectral function in $G_{RS}T_0$ and $G_{RS}T_{RS}$ can be found in the section.4 of the Supporting Information. Spectral functions from $G_0T_0@PBE$, $G_0T_0@PBE0$, $G_{RS}T_0@PBE$ and $G_{RS}T_0@PBE0$ show multiple peaks in the core region which correspond to multiple solutions in Fig.3. Spectral functions from $G_{RS}T_{RS}@PBE$ and $G_{RS}T_{RS}@PBE0$ show only one major peak, which corresponds to the correct QP state. The erroneous behavior of multiple peaks in core spectral functions was also found in G_0W_0 with commonly-used DFAs. The correct behavior in G_0W_0 can be restored by tuning up the fraction of exchange in the DFA.^{26,44}

In summary, we applied the RS Green's function in the T-Matrix method to calculate valence and core states properties. Two methods were introduced: the $G_{RS}T_0$ method that uses the RS Green's function as the reference noninteracting Green's function and the $G_{RS}T_{RS}$ method that further computes the generalized effective interaction with the the RS Green's function. $G_{RS}T_0$ and $G_{RS}T_{RS}$ methods were first examined on valence state calculations by

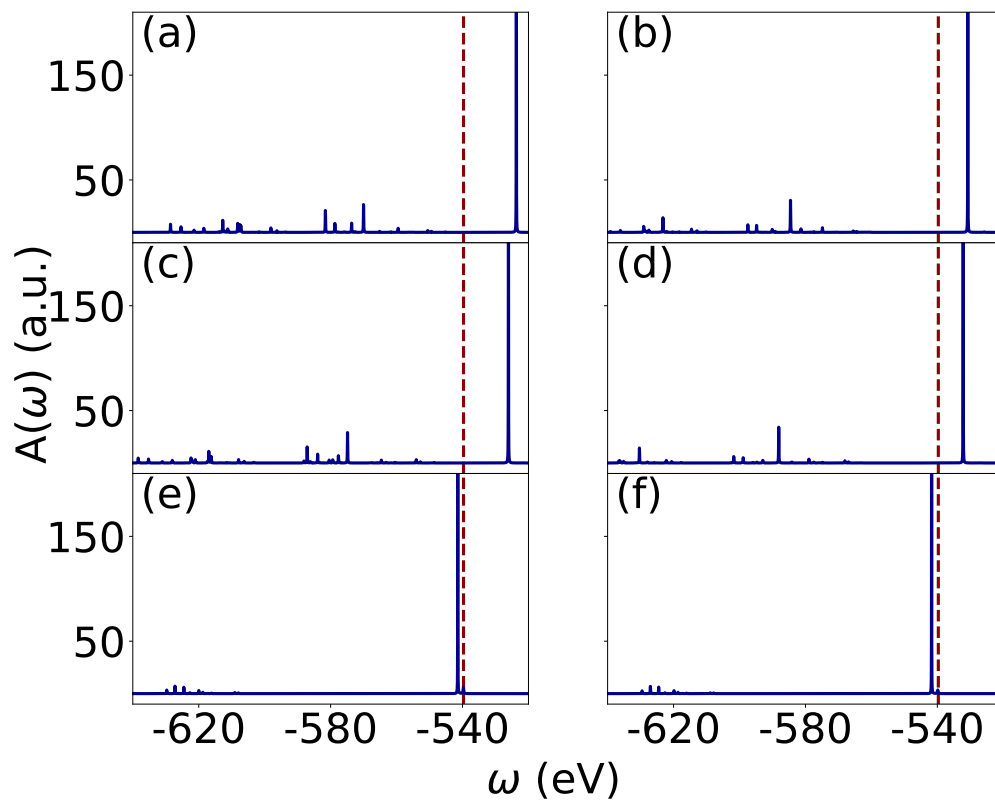


Figure 4: Spectral functions in the core region of the water molecule from (a) $G_0T_0@PBE$, (b) $G_0T_0@PBE0$, (c) $G_{RS}T_0@PBE$, (d) $G_{RS}T_0@PBE0$, (e) $G_{RS}T_{RS}@PBE$ and (f) $G_{RS}T_{RS}@PBE0$. Blue lines are spectral functions and the red line is experimental value for the CLBE. def2-TZVP basis set is used.

computing IPs in the GW100 set. It can be found that the $G_{\text{RS}}T_{\text{RS}}$ method combining with PBE and PBE0 provides accurate results with MAEs of 0.53 eV and 0.54 eV which are similar to that of $G_0T_0@HF$. However, $G_{\text{RS}}T_{\text{RS}}$ has a much smaller error spread than $G_0T_0@HF$, and thus is a more reliable method for predicting IPs. $G_{\text{RS}}T_{\text{RS}}$ also greatly reduced the starting-point dependence for IP calculations. The results on CLBES of molecules in the CORE65 set show that the $G_{\text{RS}}T_{\text{RS}}$ method greatly outperforms G_0T_0 and systematically eliminates the starting-point dependence. The improvement of $G_{\text{RS}}T_{\text{RS}}$ comes from the fact that the ppRPA excitation energies are larger, which ensures a unique solution of the QP equation in the core region. This work demonstrates the capability of the $G_{\text{RS}}T_{\text{RS}}$ method for predicting accurate QP energies for molecular systems, both for valence and for core excitations.

ACKNOWLEDGMENTS: J. L. and Z.C. acknowledge the support from the National Institute of General Medical Sciences of the National Institutes of Health under award number R01-GM061870. W.Y. acknowledges the support from the National Science Foundation (grant no. CHE-1900338).

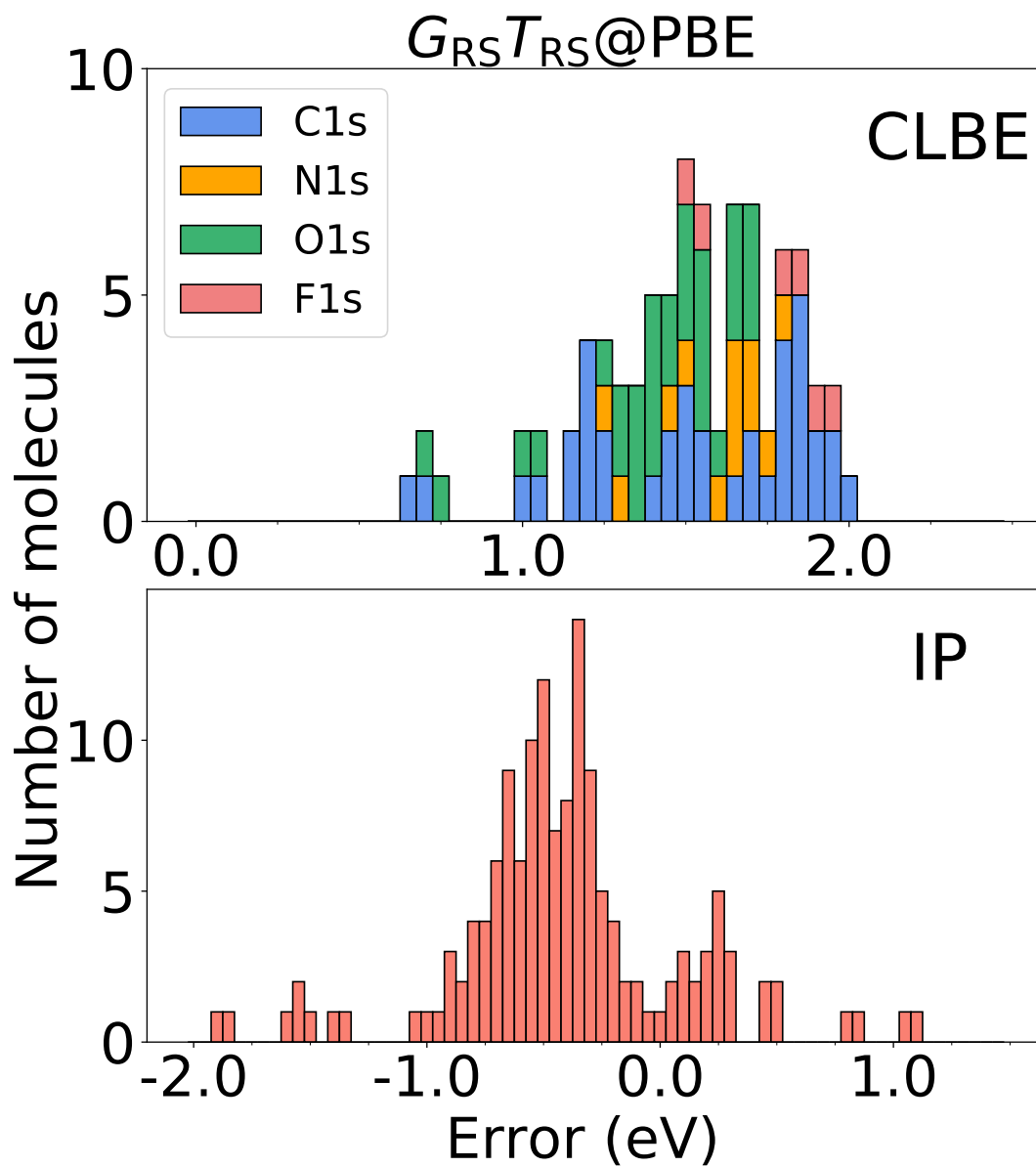


Figure 5: For Table of Contents Only”

References

- (1) Martin, R. M.; Reining, L.; Ceperley, D. M. *Interacting electrons*; Cambridge University Press, 2016.
- (2) Reining, L. The GW approximation: content, successes and limitations. *Wiley Interdisciplinary Reviews: Computational Molecular Science* **2018**, *8*, e1344.
- (3) Golze, D.; Dvorak, M.; Rinke, P. The GW compendium: A practical guide to theoretical photoemission spectroscopy. *Frontiers in chemistry* **2019**, *7*, 377.
- (4) Hedin, L. New method for calculating the one-particle Green's function with application to the electron-gas problem. *Physical Review* **1965**, *139*, A796.
- (5) Ke, S.-H. All-electron G W methods implemented in molecular orbital space: Ionization energy and electron affinity of conjugated molecules. *Physical Review B* **2011**, *84*, 205415.
- (6) Wilhelm, J.; Golze, D.; Talirz, L.; Hutter, J.; Pignedoli, C. A. Toward GW calculations on thousands of atoms. *The journal of physical chemistry letters* **2018**, *9*, 306–312.
- (7) Maggio, E.; Liu, P.; van Setten, M. J.; Kresse, G. GW 100: A plane wave perspective for small molecules. *Journal of chemical theory and computation* **2017**, *13*, 635–648.
- (8) Ren, X.; Merz, F.; Jiang, H.; Yao, Y.; Rampp, M.; Lederer, H.; Blum, V.; Scheffler, M. All-electron periodic G₀W₀ implementation with numerical atomic orbital basis functions: Algorithm and benchmarks. *Physical Review Materials* **2021**, *5*, 013807.
- (9) Caruso, F.; Rinke, P.; Ren, X.; Scheffler, M.; Rubio, A. Unified description of ground and excited states of finite systems: The self-consistent G W approach. *Physical Review B* **2012**, *86*, 081102.

- (10) Wilhelm, J.; Seewald, P.; Golze, D. Low-Scaling GW with Benchmark Accuracy and Application to Phosphorene Nanosheets. *Journal of Chemical Theory and Computation* **2021**, *17*, 1662–1677.
- (11) Caruso, F.; Atalla, V.; Ren, X.; Rubio, A.; Scheffler, M.; Rinke, P. First-principles description of charge transfer in donor-acceptor compounds from self-consistent many-body perturbation theory. *Physical Review B* **2014**, *90*, 085141.
- (12) Hellgren, M.; Caruso, F.; Rohr, D. R.; Ren, X.; Rubio, A.; Scheffler, M.; Rinke, P. Static correlation and electron localization in molecular dimers from the self-consistent RPA and g w approximation. *Physical Review B* **2015**, *91*, 165110.
- (13) Rinke, P.; Qteish, A.; Neugebauer, J.; Freysoldt, C.; Scheffler, M. Combining GW calculations with exact-exchange density-functional theory: an analysis of valence-band photoemission for compound semiconductors. *New Journal of Physics* **2005**, *7*, 126.
- (14) Rinke, P.; Janotti, A.; Scheffler, M.; Van de Walle, C. G. Defect Formation Energies without the Band-Gap Problem: Combining Density-Functional Theory and the G W Approach for the Silicon Self-Interstitial. *Physical review letters* **2009**, *102*, 026402.
- (15) Marom, N. Accurate description of the electronic structure of organic semiconductors by GW methods. *Journal of Physics: Condensed Matter* **2017**, *29*, 103003.
- (16) Jiang, H.; Gomez-Abal, R. I.; Rinke, P.; Scheffler, M. First-principles modeling of localized d states with the G W@ LDA+ U approach. *Physical Review B* **2010**, *82*, 045108.
- (17) Rinke, P.; Scheffler, M.; Qteish, A.; Winkelkemper, M.; Bimberg, D.; Neugebauer, J. Band gap and band parameters of InN and GaN from quasiparticle energy calculations based on exact-exchange density-functional theory. *Applied Physics Letters* **2006**, *89*, 161919.

- (18) Bakhsh, S.; Liu, X.; Wang, Y.; He, L.; Ren, X. Beryllium and Magnesium Metal Clusters: New Globally Stable Structures and G 0 W 0 Calculations. *The Journal of Physical Chemistry A* **2021**, *125*, 1424–1435.
- (19) Trevisanutto, P. E.; Giorgetti, C.; Reining, L.; Ladisa, M.; Olevano, V. Ab Initio G W Many-Body Effects in Graphene. *Physical review letters* **2008**, *101*, 226405.
- (20) Aguilera, I.; Vidal, J.; Wahnón, P.; Reining, L.; Botti, S. First-principles study of the band structure and optical absorption of CuGaS 2. *Physical Review B* **2011**, *84*, 085145.
- (21) Pulci, O.; Bechstedt, F.; Onida, G.; Del Sole, R.; Reining, L. State mixing for quasi-particles at surfaces: nonperturbative GW approximation. *Physical Review B* **1999**, *60*, 16758.
- (22) Blase, X.; Duchemin, I.; Jacquemin, D. The Bethe–Salpeter equation in chemistry: relations with TD-DFT, applications and challenges. *Chemical Society Reviews* **2018**, *47*, 1022–1043.
- (23) van Setten, M. J.; Caruso, F.; Sharifzadeh, S.; Ren, X.; Scheffler, M.; Liu, F.; Lischner, J.; Lin, L.; Deslippe, J. R.; Louie, S. G. et al. GW 100: Benchmarking G 0 W 0 for molecular systems. *Journal of chemical theory and computation* **2015**, *11*, 5665–5687.
- (24) Caruso, F.; Dauth, M.; van Setten, M. J.; Rinke, P. Benchmark of GW approaches for the GW 100 test set. *Journal of chemical theory and computation* **2016**, *12*, 5076–5087.
- (25) Knight, J. W.; Wang, X.; Gallandi, L.; Dolgounitcheva, O.; Ren, X.; Ortiz, J. V.; Rinke, P.; Körzdörfer, T.; Marom, N. Accurate ionization potentials and electron affinities of acceptor molecules III: a benchmark of GW methods. *Journal of chemical theory and computation* **2016**, *12*, 615–626.

- (26) Golze, D.; Rinke, P. Accurate Core-Level Spectra from GW. APS March Meeting Abstracts. 2019; pp A20–001.
- (27) Zhou, J. S.; Kas, J.; Sponza, L.; Reshetnyak, I.; Guzzo, M.; Giorgetti, C.; Gatti, M.; Sottile, F.; Rehr, J.; Reining, L. Dynamical effects in electron spectroscopy. *The Journal of chemical physics* **2015**, *143*, 184109.
- (28) Golze, D.; Wilhelm, J.; van Setten, M. J.; Rinke, P. Core-level binding energies from GW: An efficient full-frequency approach within a localized basis. *Journal of chemical theory and computation* **2018**, *14*, 4856–4869.
- (29) Hohenberg, P.; Kohn, W. Inhomogeneous electron gas. *Physical review* **1964**, *136*, B864.
- (30) Kohn, W.; Sham, L. J. Self-consistent equations including exchange and correlation effects. *Physical review* **1965**, *140*, A1133.
- (31) Parr, R.; Yang, W. Density-functional theory of atoms and molecules Oxford Univ. Press. 1989.
- (32) Marom, N.; Caruso, F.; Ren, X.; Hofmann, O. T.; Körzdörfer, T.; Chelikowsky, J. R.; Rubio, A.; Scheffler, M.; Rinke, P. Benchmark of G W methods for azabenzenes. *Physical Review B* **2012**, *86*, 245127.
- (33) Fuchs, F.; Furthmüller, J.; Bechstedt, F.; Shishkin, M.; Kresse, G. Quasiparticle band structure based on a generalized Kohn-Sham scheme. *Physical Review B* **2007**, *76*, 115109.
- (34) Kaplan, F.; Harding, M. E.; Seiler, C.; Weigend, F.; Evers, F.; van Setten, M. J. Quasiparticle self-consistent GW for molecules. *Journal of chemical theory and computation* **2016**, *12*, 2528–2541.

- (35) Caruso, F.; Rinke, P.; Ren, X.; Rubio, A.; Scheffler, M. Self-consistent G W: All-electron implementation with localized basis functions. *Physical Review B* **2013**, *88*, 075105.
- (36) Jin, Y.; Su, N. Q.; Yang, W. Renormalized singles Green's function for quasi-particle calculations beyond the G₀W₀ approximation. *The journal of physical chemistry letters* **2019**, *10*, 447–452.
- (37) Jiachen, L.; Dorothea, G.; Ye, J.; Patrick, R.; Weitao, Y. unpublished.
- (38) Szabo, A.; Ostlund, N. S. *Modern quantum chemistry: introduction to advanced electronic structure theory*; Courier Corporation, 2012.
- (39) Slater, J. C. Note on Hartree's method. *Physical Review* **1930**, *35*, 210.
- (40) Ren, X.; Tkatchenko, A.; Rinke, P.; Scheffler, M. Beyond the random-phase approximation for the electron correlation energy: The importance of single excitations. *Physical review letters* **2011**, *106*, 153003.
- (41) Ren, X.; Rinke, P.; Scuseria, G. E.; Scheffler, M. Renormalized second-order perturbation theory for the electron correlation energy: Concept, implementation, and benchmarks. *Physical Review B* **2013**, *88*, 035120.
- (42) Bruneval, F.; Marques, M. A. Benchmarking the starting points of the GW approximation for molecules. *Journal of chemical theory and computation* **2013**, *9*, 324–329.
- (43) Peng, D.; Yang, Y.; Zhang, P.; Yang, W. Restricted second random phase approximations and Tamm-Dancoff approximations for electronic excitation energy calculations. *The Journal of chemical physics* **2014**, *141*, 214102.
- (44) Golze, D.; Keller, L.; Rinke, P. Accurate absolute and relative core-level binding energies from GW. *The journal of physical chemistry letters* **2020**, *11*, 1840–1847.

- (45) Bethe, H. A.; Goldstone, J. Effect of a repulsive core in the theory of complex nuclei. *Proceedings of the Royal Society of London. Series A. Mathematical and Physical Sciences* **1957**, *238*, 551–567.
- (46) Baym, G.; Kadanoff, L. P. Conservation laws and correlation functions. *Physical Review* **1961**, *124*, 287.
- (47) Baym, G. Self-consistent approximations in many-body systems. *Physical review* **1962**, *127*, 1391.
- (48) Danielewicz, P. Quantum theory of nonequilibrium processes, I. *Annals of Physics* **1984**, *152*, 239–304.
- (49) Danielewicz, P. Quantum theory of nonequilibrium processes II. Application to nuclear collisions. *Annals of Physics* **1984**, *152*, 305–326.
- (50) Bickers, N.; Scalapino, D. Conserving approximations for strongly fluctuating electron systems. I. Formalism and calculational approach. *Annals of Physics* **1989**, *193*, 206–251.
- (51) Bickers, N.; White, S. Conserving approximations for strongly fluctuating electron systems. II. Numerical results and parquet extension. *Physical Review B* **1991**, *43*, 8044.
- (52) von Friesen, M. P.; Verdozzi, C.; Almladh, C.-O. Kadanoff-Baym dynamics of Hubbard clusters: Performance of many-body schemes, correlation-induced damping and multiple steady and quasi-steady states. *Physical Review B* **2010**, *82*, 155108.
- (53) Gukelberger, J.; Huang, L.; Werner, P. On the dangers of partial diagrammatic summations: Benchmarks for the two-dimensional Hubbard model in the weak-coupling regime. *Physical Review B* **2015**, *91*, 235114.
- (54) Romaniello, P.; Bechstedt, F.; Reining, L. Beyond the G W approximation: Combining correlation channels. *Physical Review B* **2012**, *85*, 155131.

- (55) Springer, M.; Aryasetiawan, F.; Karlsson, K. First-principles T-matrix theory with application to the 6 eV satellite in Ni. *Physical review letters* **1998**, *80*, 2389.
- (56) Guzzo, M.; Lani, G.; Sottile, F.; Romaniello, P.; Gatti, M.; Kas, J. J.; Rehr, J. J.; Silly, M. G.; Sirotti, F.; Reining, L. Valence electron photoemission spectrum of semiconductors: Ab initio description of multiple satellites. *Physical review letters* **2011**, *107*, 166401.
- (57) Zhukov, V.; Chulkov, E.; Echenique, P. GW+ T theory of excited electron lifetimes in metals. *Physical Review B* **2005**, *72*, 155109.
- (58) Noguchi, Y.; Ohno, K.; Solovyev, I.; Sasaki, T. Cluster size dependence of double ionization energy spectra of spin-polarized aluminum and sodium clusters: All-electron spin-polarized G W+ T-matrix method. *Physical Review B* **2010**, *81*, 165411.
- (59) Müller, M. C.; Blügel, S.; Friedrich, C. Electron-magnon scattering in elementary ferromagnets from first principles: Lifetime broadening and band anomalies. *Physical Review B* **2019**, *100*, 045130.
- (60) Młyńczak, E.; Müller, M.; Gospodarič, P.; Heider, T.; Aguilera, I.; Bihlmayer, G.; Gehlmann, M.; Jugovac, M.; Zamborlini, G.; Tusche, C. et al. Kink far below the Fermi level reveals new electron-magnon scattering channel in Fe. *Nature communications* **2019**, *10*, 1–5.
- (61) Liebsch, A. Ni d-band self-energy beyond the low-density limit. *Physical Review B* **1981**, *23*, 5203.
- (62) Zhang, D.; Su, N. Q.; Yang, W. Accurate Quasiparticle Spectra from the T-Matrix Self-Energy and the Particle–Particle Random Phase Approximation. *The journal of physical chemistry letters* **2017**, *8*, 3223–3227.

- (63) van Aggelen, H.; Yang, Y.; Yang, W. Exchange-correlation energy from pairing matrix fluctuation and the particle-particle random-phase approximation. *Physical Review A* **2013**, *88*, 030501.
- (64) van Aggelen, H.; Yang, Y.; Yang, W. Exchange-correlation energy from pairing matrix fluctuation and the particle-particle random phase approximation. *The Journal of chemical physics* **2014**, *140*, 18A511.
- (65) Yang, Y.; van Aggelen, H.; Steinmann, S. N.; Peng, D.; Yang, W. Benchmark tests and spin adaptation for the particle-particle random phase approximation. *The Journal of chemical physics* **2013**, *139*, 174110.
- (66) Bohm, D.; Pines, D. A collective description of electron interactions. I. Magnetic interactions. *Physical Review* **1951**, *82*, 625.
- (67) Bohm, D.; Pines, D. A collective description of electron interactions: III. Coulomb interactions in a degenerate electron gas. *Physical Review* **1953**, *92*, 609.
- (68) van Setten, M. J.; Weigend, F.; Evers, F. The GW-method for quantum chemistry applications: Theory and implementation. *Journal of chemical theory and computation* **2013**, *9*, 232–246.
- (69) Ring, P.; Schuck, P. *The nuclear many-body problem*; Springer Science & Business Media, 2004.
- (70) See <http://www.qm4d.info> for an in-house program for QM/MM simulations.
- (71) Eichkorn, K.; Treutler, O.; Öhm, H.; Häser, M.; Ahlrichs, R. Auxiliary basis sets to approximate Coulomb potentials. *Chemical physics letters* **1995**, *240*, 283–290.
- (72) Weigend, F. Accurate Coulomb-fitting basis sets for H to Rn. *Physical chemistry chemical physics* **2006**, *8*, 1057–1065.

- (73) Ren, X.; Rinke, P.; Blum, V.; Wieferink, J.; Tkatchenko, A.; Sanfilippo, A.; Reuter, K.; Scheffler, M. Resolution-of-identity approach to Hartree–Fock, hybrid density functionals, RPA, MP2 and GW with numeric atom-centered orbital basis functions. *New Journal of Physics* **2012**, *14*, 053020.
- (74) Perdew, J. P.; Burke, K.; Ernzerhof, M. Generalized gradient approximation made simple. *Physical review letters* **1996**, *77*, 3865.
- (75) Lee, C.; Yang, W.; Parr, R. G. Development of the Colle-Salvetti correlation-energy formula into a functional of the electron density. *Physical review B* **1988**, *37*, 785.
- (76) Beck, A. D. Density-functional thermochemistry. III. The role of exact exchange. *J. Chem. Phys* **1993**, *98*, 5648–6.
- (77) Adamo, C.; Barone, V. Toward reliable density functional methods without adjustable parameters: The PBE0 model. *The Journal of chemical physics* **1999**, *110*, 6158–6170.
- (78) Ernzerhof, M.; Scuseria, G. E. Assessment of the Perdew–Burke–Ernzerhof exchange–correlation functional. *The Journal of chemical physics* **1999**, *110*, 5029–5036.
- (79) Weigend, F.; Ahlrichs, R. Balanced basis sets of split valence, triple zeta valence and quadruple zeta valence quality for H to Rn: Design and assessment of accuracy. *Physical Chemistry Chemical Physics* **2005**, *7*, 3297–3305.
- (80) Weigend, F.; Häser, M.; Patzelt, H.; Ahlrichs, R. RI-MP2: optimized auxiliary basis sets and demonstration of efficiency. *Chemical physics letters* **1998**, *294*, 143–152.
- (81) Pritchard, B. P.; Altarawy, D.; Didier, B.; Gibson, T. D.; Windus, T. L. New basis set exchange: An open, up-to-date resource for the molecular sciences community. *Journal of chemical information and modeling* **2019**, *59*, 4814–4820.
- (82) Schuchardt, K. L.; Didier, B. T.; Elsethagen, T.; Sun, L.; Gurumoorthi, V.; Chase, J.;

Li, J.; Windus, T. L. Basis set exchange: a community database for computational sciences. *Journal of chemical information and modeling* **2007**, *47*, 1045–1052.

(83) Feller, D. The role of databases in support of computational chemistry calculations. *Journal of computational chemistry* **1996**, *17*, 1571–1586.